Pohjalainen, Elina; Rauhala, Taina; Valkeapää, M.; Kallioinen, J.; Kallio, Tanja

Effect of Li4Ti5O12 particle size on the performance of lithium ion battery electrodes at high C-rates and low temperatures

Published in:
Journal of Physical Chemistry C

DOI:
10.1021/jp509428c

Published: 01/01/2015

Document Version
Peer reviewed version

Please cite the original version:
Pohjalainen, E., Rauhala, T., Valkeapää, M., Kallioinen, J., & Kallio, T. (2015). Effect of Li4Ti5O12 particle size on the performance of lithium ion battery electrodes at high C-rates and low temperatures. Journal of Physical Chemistry C, 119(5), 2277-2283. https://doi.org/10.1021/jp509428c

The effect of $Li_4Ti_5O_{12}$ particle size on the performance of lithium ion battery electrodes at high C-rates and low temperatures

Elina Pohjalainen[1], Taina Rauhala[1], Markus Valkeapää[1,2], Jani Kallioinen[3], Tanja Kallio[1*]

[1]Department of Chemistry, School of Chemical Technology, Aalto University, P.O. Box 16100, FI-00076 Aalto, Finland

[2]PANalytical B.V., Linnoitustie 4 B, FI-02600 Espoo, Finland

[3]Sachtleben Pigments Oy, Titaanitie, FI-28840 Pori, Finland

[*]corresponding author; Tel: +358 50 5637 567; E-mail: tanja.kallio@aalto.fi

Abstract

Two different $Li_4Ti_5O_{12}$ materials were investigated: smaller primary particle size forming large secondary particle aggregates (LTO-SP, surface area 22 m^2/g) and larger primary particle size with less secondary particle aggregates (LTO-LP, surface area 7 m^2/g). Both samples were synthesized using the same high temperature solid state synthesis but different end processing, resulting in same crystalline structure but different particle morphology. At 0.1C measured discharge capacities were close to the theoretical capacity of $Li_4Ti_5O_{12}$ (175 mAh/g) and similar capacities were obtained at low C-rates and room temperature for both LTO-SP and LTO-LP. However, higher capacities were obtained with LTO-SP at high C-rates and -20 °C indicating beneficial effect of small particle size and large surface area. Shapes of the charge/discharge curves were different for LTO-SP and LTO-LP and this is attributed to the large surface area of LTO-SP which affects the electrochemical performance because of different reaction potentials at surface sites *vs*. bulk.

Keywords: Lithium titanate, surface area, particle morphology, rate capability, end processing

1. Introduction

Lithium titanate $Li_4Ti_5O_{12}$ (LTO) is a negative electrode material with the theoretical capacity of 175 mAh/g and high lithium insertion potential of 1.55 V (*vs.* Li/Li^+). Because of this high lithium insertion potential it is safer than traditionally used graphite negative electrode material as the possibility of lithium plating is very unlikely even at high C-rates and low temperatures. Due to the relatively low capacity and high potential the energy density of LTO is rather low. However, the possibility to use LTO with high currents makes it still ideal material for example for high power applications.

LTO has a spinel structure belonging to the $Fd\bar{3}m$ space group. In delithiated state, $Li_4Ti_5O_{12}$, the structure can be written as $(Li_3)_{8a}[Li_1Ti_5]_{16d}(O_{12})_{32e}$ where ¾ of the lithium is located at tetrahedral 8a sites, ¼ of the lithium and titanium are located at octahedral 16d sites, and oxygen is located at 32e sites. When lithium ions are inserted in the spinel structure, the inserted lithium ions occupy 16c sites and simultaneously lithium ions originally at 8a sites also migrate to 16c sites, resulting in a structure of $(Li_6)_{16c}[Li_1Ti_5]_{16d}(O_{12})_{32e}$. The volume change in the LTO unit cell during lithium insertion/extraction is very small, only 0.1-0.2 %, defining LTO as a zero strain material which causes the structural stability of LTO and predicts long cycle life for the material[1]. Lithium insertion/extraction in LTO occurs at a very constant potential over a wide range of states of charge (SOC). These flat charge/discharge profiles are typically ascribed to the two phase reaction between a lithium poor and a lithium rich LTO phase[2-4] although recently it has been stated that the phase separation only occurs on a nanometer scale[5].

Small particle size is considered advantageous for the active materials of lithium ion batteries as ionic diffusion inside active material particles is one of the key steps determining the overall performance of the battery[6]. Typically high temperature (800-1000 °C) solid state synthesis is used to produce

$Li_4Ti_5O_{12}$ resulting in relatively large particle size. Generally, high rate performance of these micronsized LTO particles is rather poor whereas nanosized LTO particles have been reported to have very high capacities with good rate capability[7]. However, nanosize also brings some disadvantages as electrodes prepared from nanosized particles usually have higher porosity and lower loading, leading to a lower energy density[7]. Larger particle surface area also increases contact resistance between particles and this might limit the performance when high C-rates and/or low operating temperatures are used[8]. In addition to this, high surface area increases the possibility for side reactions but this might not be an issue for $Li_4Ti_5O_{12}$ due to the high lithium insertion/extraction potential. Particle and electrode morphology has most pronounced effect on electrochemical performance at high currents, but also extreme temperatures are challenging. Electrochemical performance of LTO electrodes at low temperatures has not been studied extensively yet but particle size of LTO has been found to affect also low temperature performance[8, 9].

The effect of particle size of LTO on lithium ion diffusion has been examined for example by Kavan *et al.*[10]. They studied LTO particles from 9 nm to 1 µm using thin film electrodes and found that optimum performance was achieved with surface area of 100 m^2/g corresponding to a particle size of approximately 20 nm. Borghols *et al.* studied LTO particles of 12 nm and 31 nm and observed high discharge capacities exceeding the theoretical capacity of 175 mAh/g even when discharge voltage was limited to 0.9 V (*vs.* Li/Li^+)[11]. This was explained by simultaneous Li occupation at 8a and 16c sites induced by the high surface area of the nanosized particles. Thus, it is clear that in some cases nanosized materials show very different cycling behavior from similar materials in micron size. Interesting electrochemical behavior has also been observed in other nanosized electrode materials such as $LiFePO_4$ and TiO_2[12]. Reduction of the voltage plateau domain has been observed in all these materials when particle size is reduced to nanosize. In case of $LiFePO_4$ which also exhibits a two phase lithium insertion reaction this is associated with the reduction of the miscibility gap due to strain and interface energy between the end members $Li_\alpha FePO_4$ and $Li_{1-\beta}FePO_4$[13]. However, as LTO

is a zero strain material the origin of the curved voltage plateaus is different and it is suggested to result from different environments in the surface region and bulk[11].

Here we study the effect of the $Li_4Ti_5O_{12}$ particle size on the electrochemical performance at high C-rates and low temperatures. We have chosen two LTO materials manufactured by a pilot scale process with different particle size and surface area in order to study the effect of the particle morphology of LTO on the performance of lithium ion battery electrodes. Both the samples have been synthesized using the same solid state method and only the end processing is different, resulting in the same crystalline structure but somewhat different particle morphology. Thus we are also able to estimate the effect of the end treatment process in this pilot scale LTO production.

2. Experimental

Two $Li_4Ti_5O_{12}$ (LTO) active material powders (Sachtleben Pigments) manufactured by a pilot scale process were used to prepare electrodes. The most significant difference between the selected LTO samples is the particle size and therefore, these samples are hereafter referred to as LTO-SP (smaller primary particle size) and LTO-LP (larger primary particle size). The crystalline structure of the LTO samples was verified by X-ray diffraction (XRD, PANalytical X'Pert Pro, Cu $K_{\alpha 1}$ radiation). Morphology of the LTO particles and prepared electrodes was observed using scanning electron microscopy (SEM, JEOL JSM-7500FA). BET measurements were done using Nova 3200 surface area analyzer (Quantachrome Instruments).

Electrode slurries were prepared by mixing 92 m-% LTO, 3 m-% carbon black (C65, Timcal), and 5 m-% PVDF (polyvinylidene fluoride) in *N*-methyl-2-pyrrolidone (Ashland). Electrode slurries were then coated on an aluminum foil using a wet thickness of 100-250 µm to obtain desired loading.

Coated electrode foils were dried at 80 °C overnight. Electrodes with a diameter of 14 mm were cut from the dried electrode foils and calendered with a pressure of 3300 kg cm^{-2}.

Electrodes were dried overnight at 110 °C under vacuum before assembling 2016 coin cells in an argon filled glove box (oxygen and water vapour levels below 1 ppm). Lithium metal foil (0.38 mm in thickness, Aldrich) was used as a counter and reference electrode, and 1M $LiPF_6$ in ethylene carbonate:dimethyl carbonate 1:1 w/w (LP30, Merck) as an electrolyte. 260 µm thick glass microfiber filter (GF/A, Whatman) was used as a separator. Charging/discharging experiments were conducted using a Neware battery cycler. Galvanostatic charging (delithiation of LTO) and discharging (lithiation of LTO) of the half cells was done at a voltage range of 1.1 and 2.5 V *vs.* Li/Li^+ using C-rates from 0.1 C to 10 C. C-rates were calculated using the theoretical capacity of $Li_4Ti_5O_{12}$ 175 mAh g^{-1} and 1 C corresponds to complete charging or discharging in 1 hour. Low temperature measurements were conducted at 0 °C and -20 °C in a temperature chamber (Vötsch). Temperature was let to stabilize for 1h before the measurements.

Full cells against $LiFePO_4$ (LFP, commercial, surface area 13 ± 2 m^2 g^{-1}) were assembled using a similar procedure as described above for the half cells. In the full cell electrode preparation, however, the mass ratios of the electrode slurries were 86:6:8 (LTO:C:PVDF) or 80:10:10 (LFP:C:PVDF) and the thickness of the wet prints was 200 µm. The LFP coated electrode foils were dried at the room temperature overnight followed by 4 h at 80 °C in a vacuum oven. The active loadings of the 14 mm diameter electrodes were 4.7-4.8 mg cm^{-2} for LFP and 5.9-6.4 mg cm^{-2} for LTO and the electrolyte was 1M $LiPF_6$ in a 1:1 w/w mixture of ethylene carbonate and diethyl carbonate (LP40, Merck). The C-rates were calculated according to the theoretical capacity of $LiFePO_4$, 170 mAh g^{-1}, and the LTO anodes had approximately 30-40 % of excess capacity compared to the LFP electrodes. The

galvanostatic charging/discharging of the full cells was conducted between 1.0 V and 2.6 V at C-rates of 0.03 C, 0.1 C and 1 C with a 5–15 min rest between the half cycles.

Cyclic voltammetry (CV) was measured with an Autolab potentiostat (PGSTAT302N) using a Nova software. CVs were recorded within a potential range of 1.0-2.5 V (*vs.* Li/Li^+) using scan rates 0.1 mV s^{-1}, 0.2 mV s^{-1}, 0.5 mV s^{-1}, 1 mV s^{-1}, and 2 mV s^{-1}.

3. Results and Discussion

Both the LTO samples were synthesized in a pilot scale reactor using the same high temperature solid state synthesis with lithium hydroxide and titanium hydrate as precursors but different end processing. One of the end processing methods grinds the particles more intensively, resulting in smaller particle size and wider particle size distribution, while the other processing grinds the particles more lightly and thus has less pronounced effect on the particle size. The structural and morphological differences of the obtained LTO-SP powder by the more intensive grinding and LTO-LP powder by the light grinding were first examined using XRD, SEM, and BET. XRD diffractograms of LTO-SP and LTO-LP samples are presented in Supporting Information (Figure S1). Both the samples have well defined crystalline structure of $Li_4Ti_5O_{12}$ but a clear difference is observed in the intensities of the diffraction peaks, which is attributed to different crystallinity and particle size effects in the samples. A minor impurity phase observed in both the samples was confirmed to be Li_2TiO_3 by Rietveld refinement. Small amount of this Li_2TiO_3 impurity is often observed in $Li_4Ti_5O_{12}$ powders synthesized by different techniques such as solid state[14] or sol gel methods[15, 16].

SEM images of the $Li_4Ti_5O_{12}$ powders before and after the end processing (the intensive and light grinding) are presented in Figure 1. Before the end processing, LTO particles are approximately 200-250 nm in size (Figure 1a). LTO-SP after the more intensive grinding has smaller primary particle

size from some 10 nm to few hundred nanometers (Figure 1b) forming large spherical aggregates of 5-50 µm (Figure 1c). More lightly ground LTO-LP has larger primary particle size of 100-250 nm (Figure 1d) forming aggregates of 1-5 µm (Figure 1e). It is clear from the SEM images that intensive grinding as an end processing grinds the particles smaller whereas light grinding does not affect the particle size significantly. The different morphology is also shown in the BET surface areas of the $Li_4Ti_5O_{12}$ particles; 22 m^2 g^{-1} for LTO-SP and 7 m^2 g^{-1} for LTO-LP. Properties of the LTO powders are compiled in Table 1. The packing density of LTO-SP is somewhat higher than that of LTO-LP which might be beneficial for manufacturing of high density electrodes in order to obtain batteries with higher energy density. SEM image of the electrode prepared from the LTO-SP powder is presented in Supporting Information. By comparing the SEM images of the active material powders and the electrodes prepared from them it can be seen that the secondary aggregate structure is mainly preserved in the slurry mixing and electrode preparation process as flattened spherical aggregates of several tens of microns are observed in the electrode surface image of the LTO-SP electrode (Figure S2).

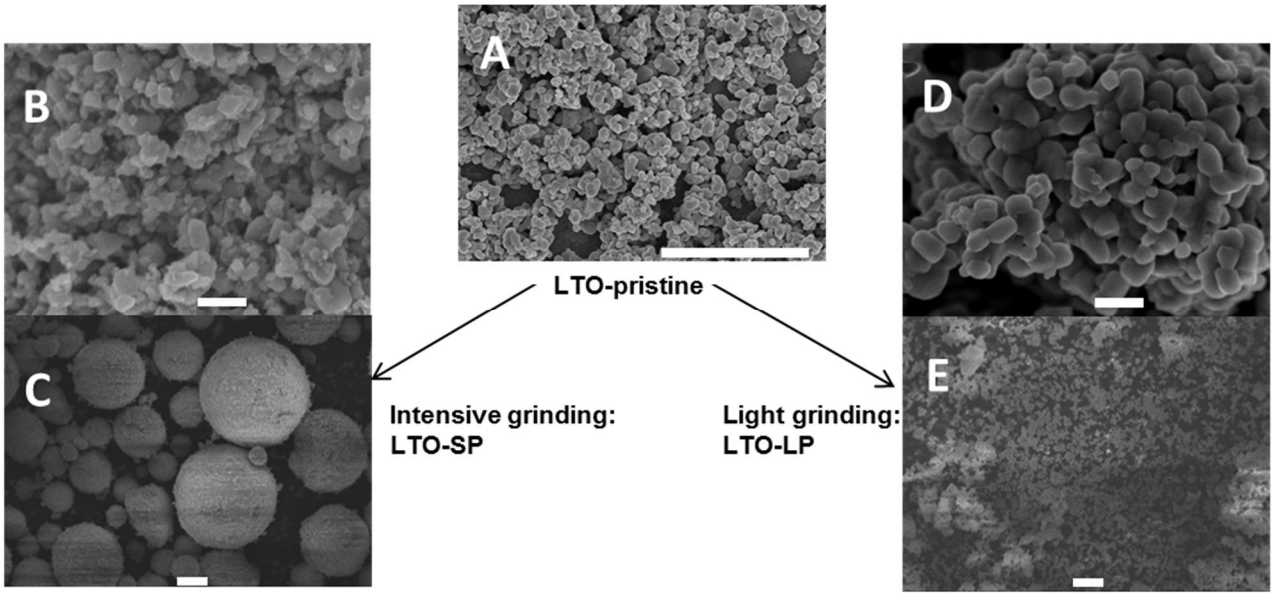

Figure 1. Scanning electron microscopy images of the $Li_4Ti_5O_{12}$ powders (a) before the end processing, LTO-pristine, (b,c) after the intensive grinding LTO-SP, and (d,e) after the light grinding LTO-LP. Scale bar in Figure a is 5 µm, in Figures b and d 500 nm, and in Figures c and e 10 µm.

Table 1. Properties of the LTO samples.

Sample	LTO-SP	LTO-LP
End process	Intensive grinding	Light grinding
Specific surface area [m^2/g]	22	7
Primary particle size [nm]	50-250	200-250
Secondary particle size [µm]	5-50	0.5-5
Tap density [g/dm^3]	970	670

Charging (delithiation of LTO) and discharging (lithiation of LTO) curves at C-rates of 0.1C…10C at the room temperature are presented in Figure 2 for both the LTO materials. Obtained capacities are close to the theoretical one at low C-rates, approximately 165-170 mAh g^{-1} at 0.1C, and 120 mAh g^{-1} or more at 10C indicating that 70% of the theoretical capacity of $Li_4Ti_5O_{12}$ is still obtained at the rather high C-rate of 10C. The capacities for LTO-SP and LTO-LP are similar at the low C-rates (less than 1C) but when C-rate is raised over 1C, the performance of LTO-SP rises above that of LTO-LP. At 10C 135 mAh/g is still obtained with LTO-SP whereas the capacity of LTO-LP remains at 120 mAh/g. This is related to the higher surface area and smaller particle size of LTO-SP as higher amount of surface sites for lithium insertion and shorter diffusion paths benefit the ability of LTO-SP to

operate at the high current. Also clear difference is observed in the shape of charge and discharge curves of the LTO-SP and LTO-LP half cells. Flat charging and discharging curves are obtained for both LTO-SP and LTO-LP with similar average charging/discharging potentials. However, whereas the flat area is extended almost over entire capacity range for LTO-LP, sloping charging and discharging curves are obtained near the end members $Li_4Ti_5O_{12}$ and $Li_7Ti_5O_{12}$ for LTO-SP as shown in Figure 2a.

Similar behavior to LTO-SP has been observed by Borghols *et al.* with significantly smaller LTO particles[11]. In addition to high capacities exceeding the theoretical capacity 175 mAh/g, sloping discharge curves were observed with 12 nm particles when compared to 31 nm particles. This was explained by different redox potentials at the near surface region *vs.* bulk. Although particles used in this study are clearly larger (primary particle size order of hundred nanometer *vs.* 12 and 31 nm in[11]), different surface areas of LTO-SP and LTO-LP, 22 m^2/g and 7 m^2/g respectively, suggest that also in this case surface effects are the main cause for the sloping charge/discharge curves observed for high surface area LTO-SP. In addition to larger surface area, LTO-SP with the smaller particle size has a higher surface to volume ratio and a wider particle size distribution (*cf.* LTO-LP). Consequently, the reactions at the near surface region have more impact on the charging and discharging processes of this electrode potentially inducing the observed curving of the (dis)charge curves as suggested in the above referred studies[11,17].

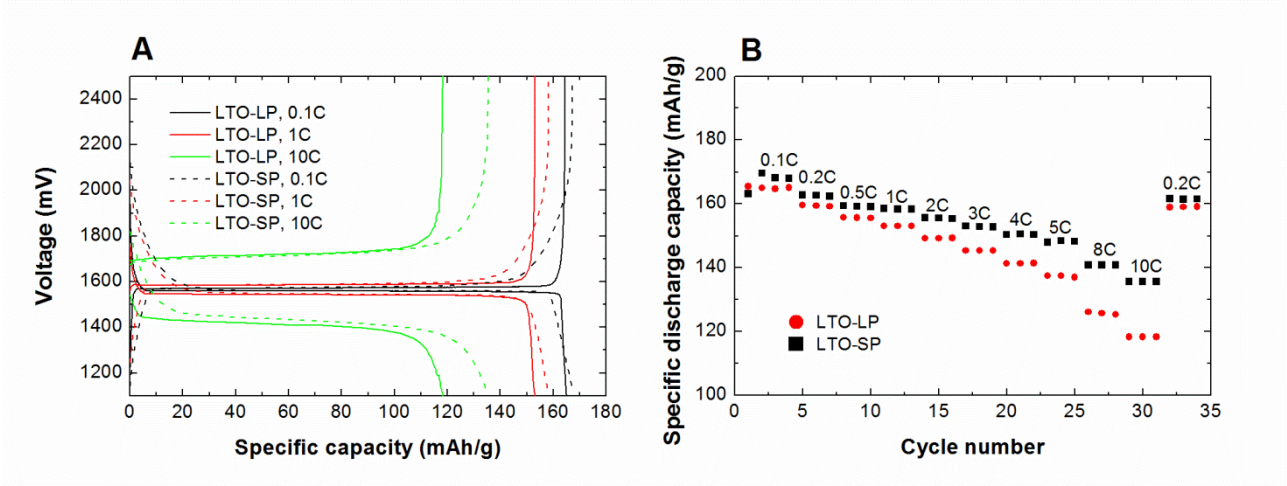

Figure 2. (a) Charge/discharge curves of the $Li_4Ti_5O_{12}$ half cells at C-rates 0.1C, 1C, and 10C at the room temperature. Solid lines represent LTO-LP and dashed lines LTO-SP. (b) Discharge capacities (lithiation of LTO) of the $Li_4Ti_5O_{12}$ half cells at C-rates 0.1C…10C as a function of cycle number at the room temperature. Black symbols represent LTO-SP and red symbols LTO-LP. Loading of the electrodes is 4.6-4.7 mg(LTO) cm^{-2}.

The effect of the surface structure of LTO has also been studied theoretically by Ganapathy and Wagemaker using DFT calculations[17]. They calculated the insertion voltages at [1 0 0], [1 1 0], and [1 1 1] surfaces and found storage properties to be strongly dependent on the surface orientation so that the insertion potential followed order [1 0 0] > [1 1 1] > [1 1 0]. Moreover, the calculated insertion voltages of the surfaces were significantly higher than the bulk voltage. Surface ratio of the surface planes can differ for LTO-SP and LTO-LP as a result of the different grinding processes. Indeed, the HRTEM images (Supporting Information Figure S3) showed lattice fringes with a d-spacing of 0.22 nm for LTO-SP and 0.48 nm for LTO-LP corresponding to the (400) and (111) planes of LTO, respectively. As the different surface planes have different lithium insertion voltages this can also affect the observed differences in the voltage profiles.

The effect of electrode architecture on the performance cannot be totally ruled out either. As the LTO-SP particles have higher packing density, it is possible that LTO-SP electrodes are also denser or form otherwise different composite structure which might benefit electronic conductivity resulting in better capacities at high C-rates. However, the difference in packing density might be evened out in the calendaring process as ohmic losses and EIS spectra (Figure S4 in Supporting Information) of the LTO-SP and LTO-LP cells are somewhat similar suggesting similar electronic conductivities. As a conclusion, the origin of the observed sloping of the (dis)charge curves remains unclear. It can result from various phenomena such as differences in the surface to bulk ratio and different reaction potentials at surface sites *vs.* bulk, accessibility of surface planes, differences in particle and electrode morphology, or combination of these.

Low temperature measurements were carried out to study more in detail the electrochemical performance of the LTO-SP and LTO-LP electrodes at demanding conditions. The charging and discharging curves of both the electrodes, LTO-SP and LTO-LP, at temperatures 20 °C, 0 °C, and -20 °C are presented in Figure 3. Capacities obtained at low current of 0.1C are similar for both LTO-SP and LTO-LP at the temperature range of -20 °C…20 °C as seen in Figure 3a. When charging/discharging current is increased to 1C (Figure 3b), capacities obtained at -20 °C are clearly higher for LTO-SP than for LTO-LP. Low conductivity of the electrolyte is one of the reasons for the capacity drop at the low temperature as EC:DMC combination is not the optimal choice for low temperature applications (ethylene carbonate is known to have a very high melting point and the freezing point of the electrolyte mixture in these experiments, 1M $LiPF_6$ in EC:DMC, is -30 °C[18]). The low conductivity of the electrolyte increases the ohmic resistance of the cell at the low temperatures thus decreasing the performance.

According to literature, electrochemical reaction step at the interface is the limiting step at low temperatures exceeding the ohmic resistance and diffusional impedance, and therefore low temperature performance can be improved by increasing the surface area of the active material particles. In that study[19], however, different electrolyte combination and a thinner Celgard separator were used. Results are still consistent with the ones in Figure 3 where LTO-SP with higher surface area shows better performance at -20 °C and high C-rate suggesting that the number of surface sites available for the (de)lithiation reactions limits the low temperature behavior also for these materials. The curving of voltage profiles observed for the LTO-SP electrodes at the room temperature is also detected at all the studied temperatures indicating that the phenomenon or phenomena inducing the curving are not attenuated by the decrease of the temperature.

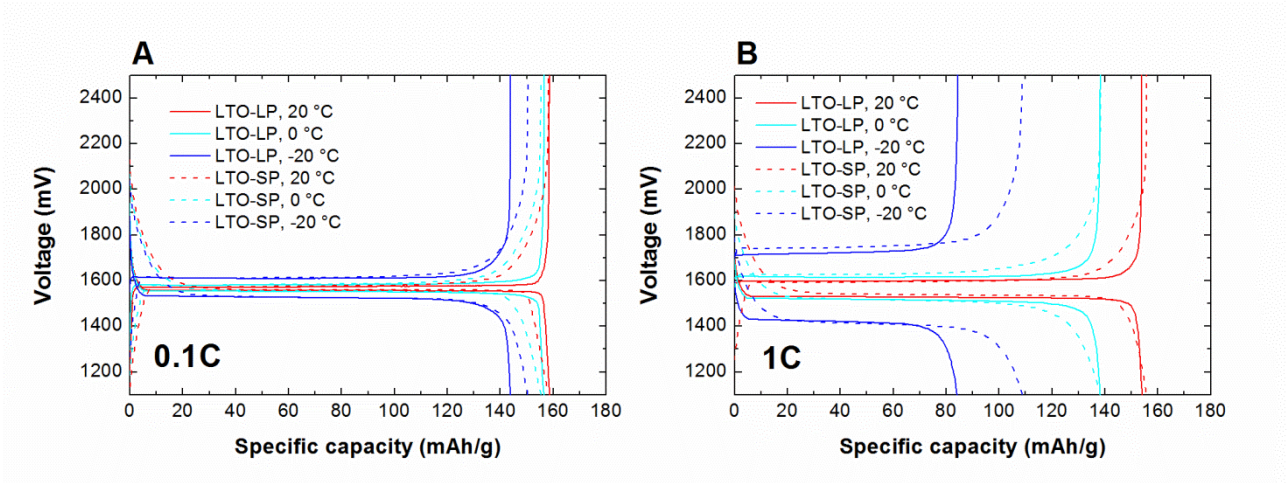

Figure 3. Charge/discharge curves of the $Li_4Ti_5O_{12}$ half cells at C-rates 0.1C (a) and 1C (b) at the temperatures of 20 °C, 0 °C, and -20 °C. Solid lines represent LTO-LP and dashed lines LTO-SP.

LTO-SP showing higher capacities was chosen for longer measurements to study the effect of the low temperature on the cycle life of LTO electrodes. No change in the cycling behavior was observed at the room temperature after the measurements at the lower temperatures with the half cells, and this was confirmed with the LFP-LTO full cells. The full cells were first cycled for 20 charge/discharge cycles either at the room temperature or at -20 °C at a C-rate of 1C followed by 300 cycles at the

room temperature. No differences in the cycle life or the shape of the charge/discharge curves were observed between the cells cycled only at the room temperature and the cells cycled first at -20 °C, as shown in Figure 4 and Figure S5 in Supporting Information. This result indicates that no significant structural changes take place in LTO during cycling at -20 °C and thus highlights the suitability of both LTO and LFP electrodes for low temperature applications.

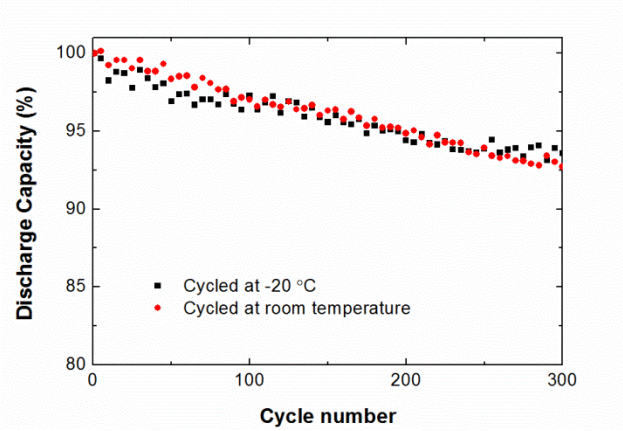

Figure 4. The room temperature cycle life of $LiFePO_4$/1 M $LiPF_6$ in EC:DEC (1:1)/$Li_4Ti_5O_{12}$ cells after 20 charge/discharge cycles at the C-rate 1C at -20 °C (black) or at room temperature (red). The discharge capacity (corresponding here to the delithiation of $Li_4Ti_5O_{12}$) is normalized with the capacity of the first room temperature cycle after 20 cycles at -20 °C or at the room temperature, which was 135-140 mAh g^{-1} (relative to the active mass of $LiFePO_4$) for the cells charged/discharged at either temperature.

Cyclic voltammograms of the LTO-SP and LTO-LP electrodes are presented in Figure 5. In both the LTO samples peak heights as well as peak widths increase as the scan rate v is increased, and the increase in the peak maximum as a function of square root of scan rate $v^{1/2}$ is linear indicating that the lithium ion (de)insertion reaction is mass transfer controlled. Somewhat higher peaks are observed for LTO-LP than for LTO-SP but integrated peak areas corresponding the capacities of the samples are similar (approximately 160 mAh/g at the scan rate of 0.1 mV/s). The most obvious difference

between the peaks of these samples is observed in the shape of the peaks which are narrower for LTO-LP, the material with the lower surface area (see Table 1). This is most clearly seen in the high voltage end of the cathodic and anodic peaks, in other words in the region where x in $Li_{4+x}Ti_5O_{12}$ is close to zero, when reactions and transport is expected to take place at the near surface region of the particles. As for the discharging curves of the half cells (see Figures 2 and 3), the cathodic peak currents of CVs show clearly that the lithium insertion starts at a higher potential for LTO-SP indicating higher activity of this material. The sloping of the anodic peak in the CVs becomes more pronounced for the high surface area LTO-SP with the increasing scan rate suggesting sluggish delithiation process when most of the lithium is removed though the diffusion lengths for lithium ions are lower in this material in comparison to LTO-LP. These results suggest that the sloping results from the above discussed differences in the lithium (de)insertion voltages or occupation of different surface sites. Once again the results highlight that the surface region has an important role on the lithium (de)insertion reaction and that the end treatment affects notably on the performance of LTO. Electrochemical modelling of transport and kinetics of the lithium (de)insertion reactions on porous LTO electrodes would give further information on the observed phenomena but is out of scope of this study because of the complexity of that kind of a model.

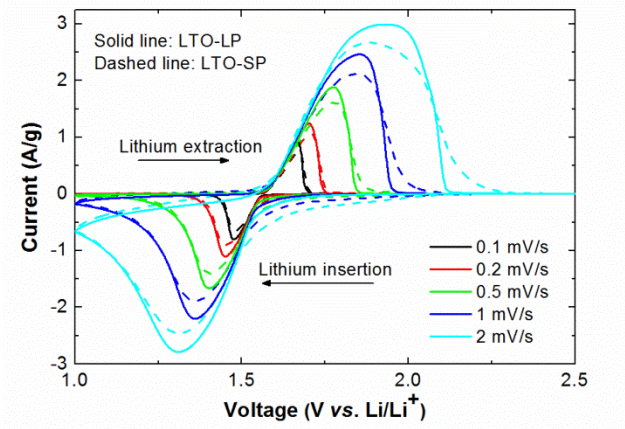

Figure 5. Cyclic voltammograms of the LTO-SP and LTO-LP half cells using scan rates 0.1 mV s^{-1} … 2 mV s^{-1}. Solid lines represent LTO-LP and dashed lines LTO-SP.

Open circuit voltages of LTO-SP and LTO-LP after discharge of the half cells *i.e.* at the lithiated state are presented in Figure 6. It is clear that both samples LTO-SP and LTO-LP saturate to the same voltage value of 1.56 V *vs.* Li/Li^+ but the time scale for the relaxation process is quite different. For LTO-LP, saturation voltage is reached in some hours whereas for LTO-SP the relaxation takes several weeks. Borghols *et al.* investigated the effect of particle size for LTO particles of <50 nm and stated that smaller particles show larger capacities because of simultaneous occupation of 8a and 16c sites and this simultaneous accommodation is more favorable in the surface region than in the bulk[11]. Here we suggest that when discharged to 1.1 V overlithiated phase $Li_{7+x}Ti_5O_{12}$ is formed on the surface of the particles and this is more clearly seen in the LTO-SP particles with the high surface area. In the bulk of the particle $Li_4Ti_5O_{12}/Li_7Ti_5O_{12}$ phases are still present and simultaneous occupation of 8a and 16c sites on the surface might block further diffusion of lithium into the bulk[20]. After long relaxation time overlithiated phase $Li_{7+x}Ti_5O_{12}$ on the surface and $Li_4Ti_5O_{12}/Li_7Ti_5O_{12}$ phases in the bulk are relaxed again into $Li_4Ti_5O_{12}$ and $Li_7Ti_5O_{12}$ phases[20]. This relaxation process takes the longer time the more overlithiated phase there exists as seen in the OCP curves of LTO-SP and LTO-LP in Figure 6.

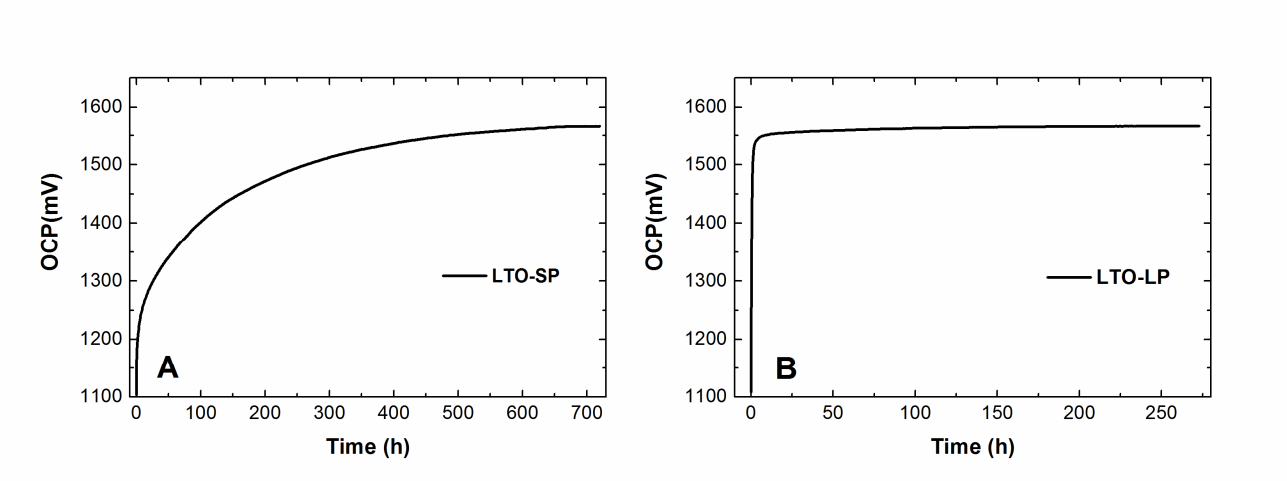

Figure 6. OCP curves after discharge of the half cells to lithiated state for the (a) LTO-SP and (b) LTO-LP cells.

As a summary, qualitatively different behavior during charging/discharging and equilibration processes has been shown for LTO materials synthetized using the same process. These results suggest that the observed difference in the behavior of the studied LTO-SP and LTO-LP samples originates besides from the trivial particle size effect also from different particle morphology of the samples induced by the different grinding process. The observed differences in behavior between LTO-SP and LTO-LP during dynamic and equilibrium conditions suggest that (de)lithiation process is different because of the available surface sites and crystal planes inducing different activity for (de)lithiation processes and/or, because of overlithiation of the near surface region of LTO. However, the electrode morphology is known to affect lithium ion (de)insertion reaction and its effect cannot be completely ruled out. In any case, this study highlights that particle size and morphology of the active material has an important role in (dis)charging lithium ion batteries. To further study the origin and the factors affecting the (dis)charging behavior a detailed electrochemical model including kinetics and transportation in porous electrode is under development.

4. Conclusions

Two different end milling processes were investigated for LTO pilot scale production; more intensive grinding (LTO-SP) and light grinding (LTO-LP). Intensive grinding was found out to be more feasible end processing technique as it produces $Li_4Ti_5O_{12}$ crystals with smaller primary particle size and larger surface area enabling to store more lithium at extreme conditions. Performance of LTO-SP and LTO-LP was similar at low C-rates at the room temperature. However, obtained capacities of LTO-SP were higher at high C-rates and at low temperature. Difference in the measured capacities at high C-rates and low temperatures, and different shapes of charge/discharge curves of LTO-SP and LTO-LP and different time range for reaching equilibrium were attributed to surface effect *i.e.* higher reaction voltage of the surface sites *vs.* bulk and, overlithiation of the surface sites near fully lithiated

state. These half cell measurements suggest that the phenomena at surface region have a significant role in lithium intercalation and deintercalation near the end members $Li_4Ti_5O_{12}$ and $Li_7Ti_5O_{12}$ i.e. when LTO has very low or high lithium ion content. However, to understand the origin of the observed differences modelling of the electrochemical measurement data is going on.

Acknowledgement

Tekes is thanked for financial support. This work made use of the Aalto University Nanomicroscopy Center (Aalto-NMC) premises. Mr. Mikko Nisula, Dr. Eeva-Leena Rautama and Dr. A. Santasalo-Aarnio are acknowledged for helpful scientific discussions.

Supporting information available: XRD diffractograms, SEM image of the LTO-SP electrode, EIS spectras of LTO-SP and LTO-LP electrodes, and low temperature charge/discharge curves of LTO/LFP full cells are presented in Supporting information. This material is available free of charge via the Internet at http://pub.acs.org

References

(1) Ariyoshi, K.; Yamato, R.; Ohzuku, T. Zero-Strain Insertion Mechanism of Li[Li1/3Ti5/3]O4 for Advanced Lithium-Ion (Shuttlecock) Batteries. Electrochim. Acta 2005, 51, 1125-1129.

(2) Lu, X.; Zhao, L.; He, X.; Xiao, R.; Gu, L.; Hu, Y.; Li, H.; Wang, Z.; Duan, X.; Chen, L. et al. Lithium Storage in Li4Ti5O12 Spinel: The Full Static Picture from Electron Microscopy. Adv Mater 2012, 24, 3233-3238.

(3) Kitta, M.; Akita, T.; Tanaka, S.; Kohyama, M. Characterization of Two Phase Distribution in Electrochemically-Lithiated Spinel Li4Ti5O12 Secondary Particles by Electron Energy-Loss Spectroscopy. J. Power Sources 2013, 237, 26-32.

(4) Scharner, S.; Weppner, W.; Schmid-Beurmann, P. Evidence of Two-Phase Formation upon Lithium Insertion into the Li1.33Ti1.67O4 Spinel. J. Electrochem. Soc. 1999, 146, 857-861.

(5) Wagemaker, M.; van Eck, Ernst R. H.; Kentgens, A. P. M.; Mulder, F. M. Li-Ion Diffusion in the Equilibrium Nanomorphology of Spinel Li4+xTi5O12. J. Phys. Chem. B 2009, 113, 224-230.

(6) Gaberscek, M.; Dominko, R.; Jamnik, J. Is Small Particle Size More Important than Carbon Coating? an Example Study on LiFePO4 Cathodes. Electrochem. Commun. 2007, 9, 2778-2783.

(7) Chen, Z.; Belharouak, I.; Sun, Y.; Amine, K. Titanium-Based Anode Materials for Safe Lithium-Ion Batteries. Adv. Funct. Mater. 2013, 23, 959-969.

(8) Allen, J. L.; Jow, T. R.; Wolfenstine, J. Low Temperature Performance of Nanophase Li4Ti5O12. J. Power Sources 2006, 159, 1340-1345.

(9) Yuan, T.; Yu, X.; Cai, R.; Zhou, Y.; Shao, Z. Synthesis of Pristine and Carbon-Coated Li4Ti5O12 and their Low-Temperature Electrochemical Performance. J. Power Sources 2010, 195, 4997-5004.

(10) Kavan, L.; Procházka, J.; Spitler, T. M.; Kalbáč, M.; Zukalová, M.; Drezen, T.; Grätzel, M. Li Insertion into Li4Ti5O12 (Spinel) : Charge Capability Vs. Particle Size in Thin-Film Electrodes. J. Electrochem. Soc. 2003, 150, A1000-A1007.

(11) Borghols, W. J. H.; Wagemaker, M.; Lafont, U.; Kelder, E. M.; Mulder, F. M. Size Effects in the Li4+xTi5O12 Spinel. J. Am. Chem. Soc. 2009, 131, 17786-17792.

(12) Wagemaker, M.; Mulder, F. M. Properties and Promises of Nanosized Insertion Materials for Li-Ion Batteries. Acc. Chem. Res. 2013, 46, 1206-1215.

(13) Kobayashi, G.; Nishimura, S.; Park, M.; Kanno, R.; Yashima, M.; Ida, T.; Yamada, A. Isolation of Solid Solution Phases in Size-Controlled LixFePO4 at Room Temperature. Adv. Funct. Mater. 2009, 19, 395-403.

(14) Prakash, A. S.; Manikandan, P.; Ramesha, K.; Sathiya, M.; Tarascon, J.; Shukla, A. K. Solution-Combustion Synthesized Nanocrystalline Li4Ti5O12 as High-Rate Performance Li-Ion Battery Anode. Chem. Mater. 2010, 22, 2857-2863.

(15) Mani, J.; Katzke, H.; Habouti, S.; Moonoosawmy, K. R.; Dietze, M.; Es-Souni, M. A Template-Free Synthesis and Structural Characterization of Hierarchically Nano-Structured Lithium-Titanium-Oxide Films. J. Mater. Chem. 2012, 22, 6632-6638.

(16) Pang, W. K.; Sharma, N.; Peterson, V. K.; Shiu, J.; Wu, S. In-Situ Neutron Diffraction Study of the Simultaneous Structural Evolution of a LiNi0.5Mn1.5O4 Cathode and a Li4Ti5O12 Anode in a LiNi0.5Mn1.5O4||Li4Ti5O12 Full Cell. J. Power Sources 2014, 246, 464-472.

(17) Ganapathy, S.; Wagemaker, M. Nanosize Storage Properties in Spinel Li4Ti5O12 Explained by Anisotropic Surface Lithium Insertion. ACS Nano 2012, 6, 8702-8712.

(18) Plichta, E. J.; Behl, W. K. A Low-Temperature Electrolyte for Lithium and Lithium-Ion Batteries. J. Power Sources 2000, 88, 192-196.

(19) Abraham, D. P.; Heaton, J. R.; Kang, S.-H.; Dees, D. W.; Jansen, A. N. Investigating the Low-Temperature Impedance Increase of Lithium-Ion Cells. J. Electrochem. Soc. 2008, 155, A41-A47.

(20) Choi, Z.; Kramer, D.; Mönig, R. Correlation of Stress and Structural Evolution in Li4Ti5O12-Based Electrodes for Lithium Ion Batteries. J. Power Sources 2013, 240, 245-251.

Supporting Information

The effect of $Li_4Ti_5O_{12}$ particle size on the performance of lithium ion battery electrodes at high C-rates and low temperatures

Elina Pohjalainen[1], Taina Rauhala[1], Markus Valkeapää[1,2], Jani Kallioinen[3], Tanja Kallio[1*]

[1]Department of Chemistry, School of Chemical Technology, Aalto University, P.O. Box 16100, FI-00076 Aalto, Finland

[2]PANalytical B.V., Linnoitustie 4 B, Espoo, Finland

[3]Sachtleben Pigments Oy, Titaanitie, FI-28840 Pori, Finland

[*]corresponding author; Tel: +358 50 5637 567; E-mail: tanja.kallio@aalto.fi

To show details enlarged XRD diffractograms of the LTO-LP and LTO-SP samples are shown in Figure S1 with an inset showing the peak [400].

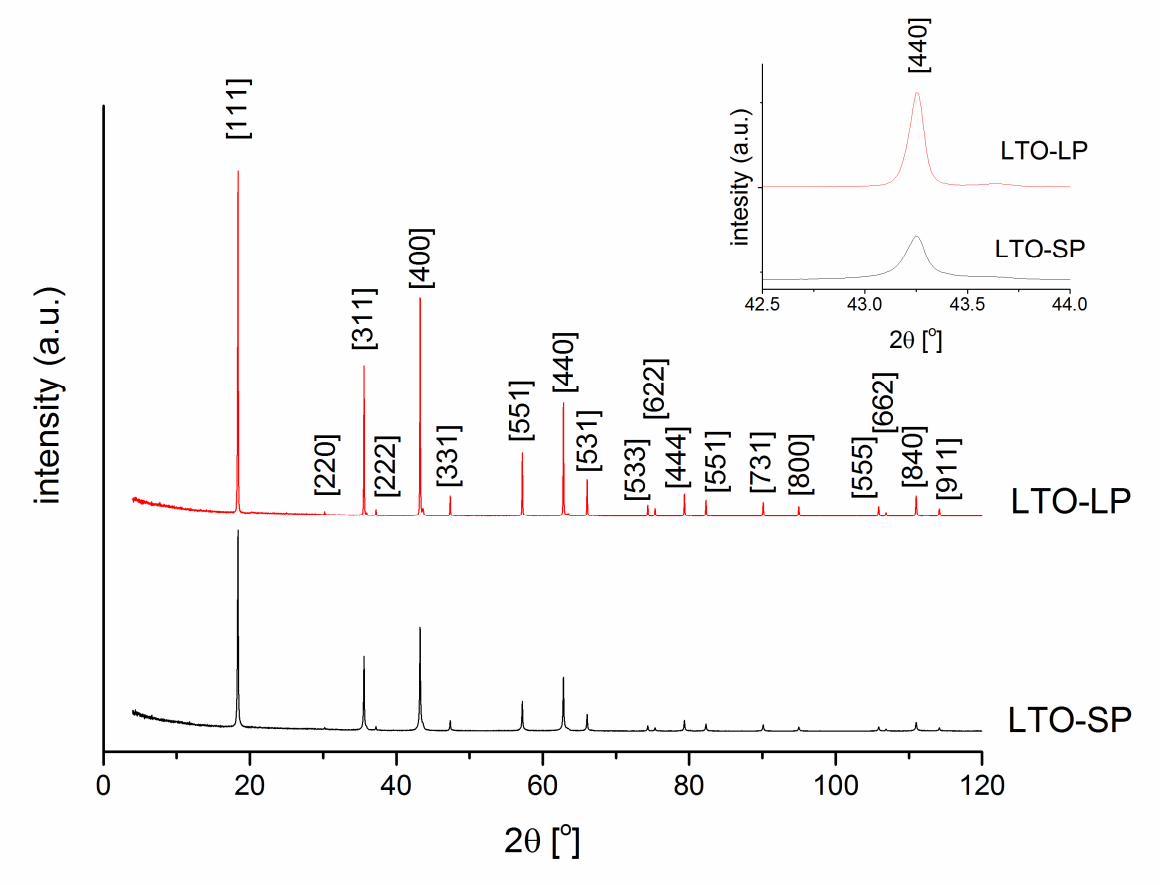

Figure S1. XRD diffractograms of the LTO-LP and LTO-SP samples.

SEM image of the LTO-SP electrode is presented in Figure S2. Secondary aggregate structures are clearly visible as the surface consists of flattened spheres of 10-30 µm.

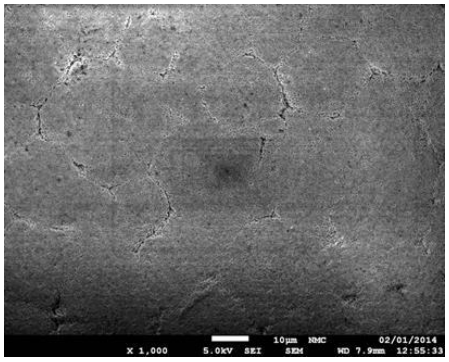

Figure S2. A scanning electron microscopy image of the investigated LTO-SP electrode.

High-resolution Transmission electron microscopy (HRTEM) was used to obtain the particle morphology by using a double-aberration corrected JEOL 2200FS (JEOL, Japan) microscope equipped with a field emission gun (FEG) operated at 200kV.

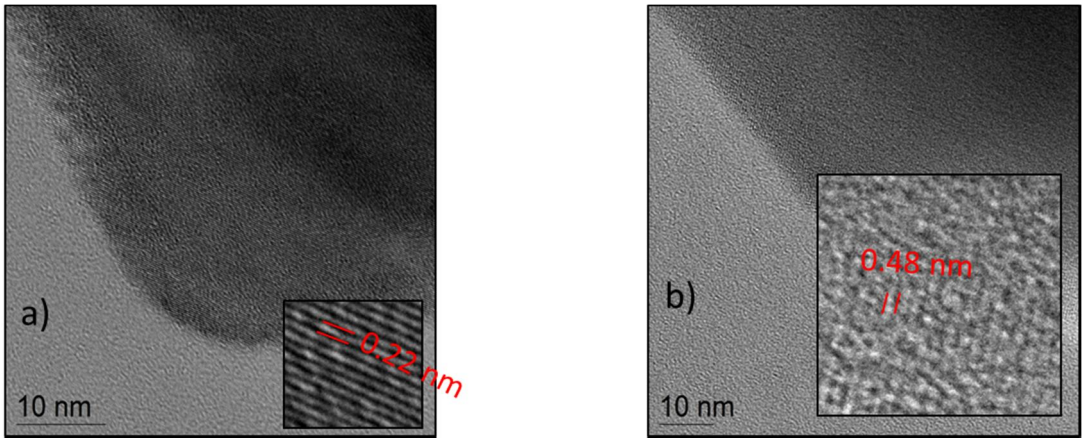

Figure S3. HRTEM images the investigated a) LTO-SP and b) LTO-LP samples.

Electrochemical impedance spectroscopy (EIS) was performed to study if there was any difference observed in electrical conductivity of the prepared electrodes. Measurement was conducted with an Autolab potentiostat (PGSTAT302N) using 3-electrode set up (Hohsen HS-3E test cell) with lithium metal foil counter and reference electrodes. Frequency range of 100 kHz – 0.01 Hz and voltage amplitude of 10 mV were used. No clear difference was observed in the measured EIS spectras between LTO-SP and LTO-LP as presented in Figure S4 indicating similar electric conductivity for both the electrodes.

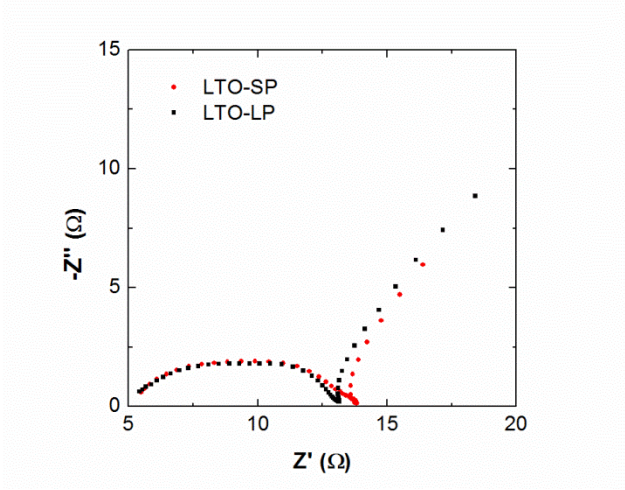

Figure S4. EIS spectras of the LTO-SP and LTO-LP electrodes.

Charge/discharge curves of $LiFePO_4/Li_4Ti_5O_{12}$ full cell at the room temperature and -20 °C are presented in Figure S5. LTO electrode was manufactured using LTO-SP. The full cells were first charged at room temperature at a C-rate 1C, then cooled to -20 °C and discharged and cycled for 20 cycles. No difference in the shape of the charge/discharge curves at the room temperature was observed before (black curves) and after (green curves) the 20 cycles at -20 °C. Also the capacity during the low temperature cycles stayed constant or was slightly increasing probably due to internal heating of the cell.

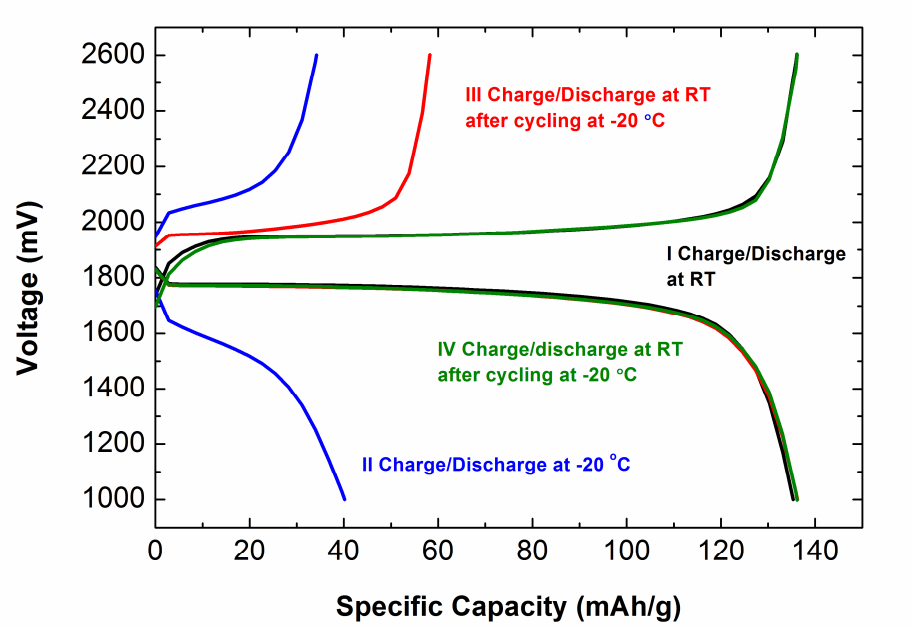

Figure S5. Charge/discharge curves of $LiFePO_4$/1 M $LiPF_6$ in EC:DEC (1:1)/$Li_4Ti_5O_{12}$ cell at different temperatures at the C-rate 1C. The initial room temperature charge/discharge curves are presented in black and the first cycle at -20 °C is plotted in blue. The red and green curves correspond to the first and second post-characterization curves at the room temperature, respectively.